Tellus (1986), *38B*, 285–299

The removal of soluble species by warm stratiform clouds

By YU QIN* and W. L. CHAMEIDES, *School of Geophysical Sciences, Georgia Institute of Technology, Atlanta, Ga. 30332, USA*

(Manuscript received October 14, 1985; in final form April 1, 1986)

ABSTRACT

A one-dimensional, time-dependent model has been developed to study the removal of soluble gases from a warm, precipitating stratiform cloud. The model calculates the distributions of water vapor and condensed water, in the form of cloud drops and raindrops, as well as the in-cloud concentration of a soluble species in the gas and aqueous phases for a specified profile of pressure and temperature and an assumed updraft velocity. Highly soluble gases are found to be rapidly dissolved into cloud droplets and then slowly incorporated into raindrops as cloudwater is converted to rainwater. As this rainwater begins to fall out of the cloud, the total in-cloud abundance of highly soluble species rapidly decreases, causing the rate of removal of the species from the cloud to also decrease. The rate of removal of highly soluble species continues to decrease until a balance between loss via rainout and transport of new material into the cloud is reached, and an approximate steady state is established. Thus the rainout rate for highly soluble species is found to be ultimately limited by the rate at which new gaseous material can be transferred from the cloud-free air into the cloud. The model calculations indicate that turbulence represents an important mechanism by which highly soluble gases are transported into stratiform clouds and thus the calculated rate of removal of highly soluble species from these types of clouds is dependent on the parameterization chosen to simulate this process.

1. Introduction

Because of the high levels of condensed water typically found in clouds, they represent a unique chemical environment in the atmosphere. When an air mass is entrained into a cloud, the soluble species are rapidly separated from the insoluble ones and dissolved in the liquid water drops, contained in the cloud. Removal of these soluble species from the atmosphere via rainout occurs when the water containing dissolved constituents falls out of the cloud as raindrops and collects on the earth's surface. For some of the elements in the atmosphere (most notably reactive N and S) rainout represents one of the most important mechanisms of removal from the atmosphere (c.f. Chameides and Davis, 1982) and, as a result, a quantitative understanding of physical and chemical processes which control the rate of atmospheric rainout-removal is highly desirable.

Thus far studies of the removal of soluble gases by clouds have focussed on the transfer of gases to cloud droplets. Because the kinetic processes controlling this transfer (i.e., molecular diffusion to a droplet surface followed by dissolution) occur relatively rapidly, it has been concluded that the partitioning of a soluble species within a cloud between the gas and aqueous phase is often solely determined by a thermodynamic equilibrium involving the species' solubility in liquid water (c.f. Hales, 1982; Sarma, 1983; Chameides, 1984). On the basis of this result, it has been further inferred that rainout of a soluble species is controlled by the same thermodynamic partitioning (Brimblecombe and Dawson, 1984; Giorgi and Chameides, 1984). However, all of these previous studies ignored the effects that cloud microphysics and dynamics might have on this partitioning. In this work we report on calcula-

* Visiting Scholar from Department of Geophysics, Peking University, Beijing, China.

tions which investigate the impact these other physical processes may have on the partitioning of a soluble gas between the gas and aqueous phases and thus on the removal rate of gaseous species from clouds.

To carry out this investigation, we have developed a one-dimensional model of a warm, precipitating, stratiform cloud which simulates the relevant dynamical and microphysical processes that lead to the production of cloudwater and its subsequent conversion to rainwater. To this model we have added mass-continuity equations describing the reversible transfer of a gaseous species to cloudwater and then to rainwater. While the model represents a highly simplified and idealized picture of a stratiform cloud, we believe that it captures enough of the essence of cloud physics to indicate in a semi-quantitative fashion how these processes might affect the removal of soluble species from clouds and thus point to areas that require further study.

In Section 2, we describe the cloud physics model used in our calculations to simulate the dynamical and microphysical processes of a stratiform cloud. We then discuss the use of this model to study the scavenging of a soluble species from the gas phase, its incorporation into cloud- and rainwater, and its eventual removal from the cloud via rainout.

2. Cloud physics

2.1. Physical model description

The physics of a warm stratiform cloud are simulated with the one-dimensional, time-dependent model of Hu et al. (1983a, b). This model is similar to those of Kessler (1969), Berry (1968), and Simpson and Wiggert (1969), in that it treats the complex microphysical processes controlling cloud droplet and raindrop formation through a number of simplifying parameterizations. Assuming horizontal homogeneity and a constant updraft velocity, W, the concentrations of liquid water and water vapor are determined in the model as a function of time and height above cloud base (i.e., $z = 0$) for specified profiles of pressure, p, and temperature, T. Fig. 1 depicts the distributions of p and T adopted in the calculations presented here; also shown is the saturated water vapor-mixing ratio, Q_{VS}, as a function of height obtained from these profiles.

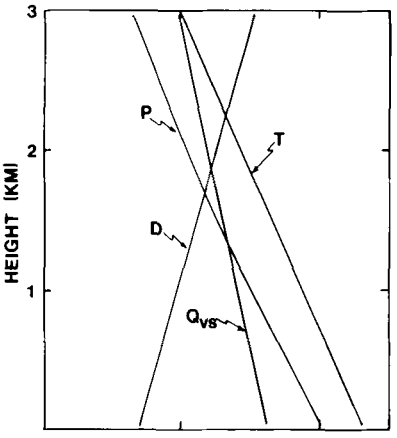

Fig. 1. Profiles of pressure, P, temperature, T, saturated water vapor mixing ratio, Q_{VS}, and molecular diffusion coefficient, D adopted in the model calculations. Note that T was assumed to be pseudo-adiabatic and D was obtained from the formula given by Pruppacher and Klett (1978).

For a warm cloud, three kinds of water must be considered: water vapor, cloudwater, and rainwater. The mass-continuity equations describing the local time rate of change in the mass mixing ratios of these three parameters (i.e., Q_V, Q_C, and Q_R) are given by (1):

$$\partial Q_V/\partial t = -W\,\partial Q_V/\partial z - \text{CONDC} - \text{CONDR} + K\,\partial^2 Q_V/dz^2, \quad (1a)$$

$$\partial Q_C/\partial t = -W\,\partial Q_C/\partial z + \text{CONDC} - \text{COLL} - \text{AUTO} + K\,\partial^2 Q_C/dz^2, \quad (1b)$$

$$\partial Q_R/\partial t = -(W-U)\,\partial Q_R/\partial z + \text{CONDR} - \text{COLL} + \text{AUTO} + K\,\partial^2 Q_R/dz^2, \quad (1c)$$

where CONDC is the rate of condensation of water vapor into cloudwater, CONDR is the rate of condensation into rainwater, COLL is the rate at which cloudwater is converted into rainwater by collision and coalescence, AUTO is the rate of conversion by so-called autoconversion processes, K is the eddy diffusion-coefficient, and U is the

group terminal velocity for raindrops. (Note that clouddrops are assumed to have negligibly small fall velocities and they hence travel with a vertical velocity equal to the updraft velocity of the air.)

One of the terms of interest in (1) is that due to eddy diffusion. Because of the much weaker vertical updrafts and hence smaller vertical extents of stratiform clouds, turbulent transport, especially that involving a transfer between the cloud and the outside air, can be quite important (c.f. Best, 1952: Mason, 1960). To simulate this effect we have adopted the standard eddy diffusion parameterization with the transport assumed to be proportional to the eddy-diffusion coefficient K. In the Standard Model, we have taken K to be equal to 20 m^2/s (Khrgian, 1961; Hu et al., 1983a), however, sensitivity calculations with K equal to 40 m^2/s have also been carried out and will be presented. As will be illustrated later, the solution for the water-related parameters (Q_V, Q_C, and Q_R) is relatively insensitive to this factor of 2 variations in K. On the other hand, the calculated rate of removal of a highly soluble trace species from the cloud will be shown to be quite sensitive to variations in this parameter.

Because cloud and rain drops are typically distributed over a wide range of radii, (1) involves a cumbersome series of integrals over the cloud and rain drop size distributions and is, therefore, quite difficult to solve. Instead of treating this complex problem, we simplify the problem considerably by parameterizing the various processes in (1) in terms of a single representative radius, R_C for cloudwater and R_R for rainwater. As noted above these parameterizations are quite similar to those adopted by previous investigators.

In the case of cloud water we assume a monodisperse distribution with constant total concentration of droplets, N_C, equal to 10^8 m^{-3}. Then R_C, is given by

$$R_C = (3\rho_a Q_C / N_C^4 \pi \rho_W)^{1/3}, \tag{2}$$

where ρ_a and ρ_W are the densities of air and water, respectively. Although not specifically indicated in (2), since Q_C varies with both time and height, R_C is also a function of t and z. Also note that by taking N_C to be a constant and coalescence, we are effectively assuming that a source of cloud drops exists at all times and levels which is exactly equal to the rate at which cloud drops are converted into raindrops.

In the case of rainwater, the total concentration of drops, N_R, is allowed to vary as a function of time according to (3)

$$\partial N_R/\partial t = -(U - W)\,\partial N_R/\partial z + \text{AUTON} + K\partial^2 N_R/\partial z^2, \tag{3}$$

where AUTON is the rate of production of new raindrops by auto conversion. Assuming that auto conversion produces drops with an initial radius of $R_o = 40$ μm, it follows that

$$\text{AUTON} = \text{AUTO}/(4/3\,\pi R_o^3\,\rho_W/\rho_a) \tag{4}$$

For the raindrop sizes, we assume a Marshall-Palmer distribution (Marshall and Palmer, 1948), so that $dn(D)$, the total number of raindrops with diameters between D and $D + dD$ is given by

$$dn(D) = N_{RO} \exp(-\Lambda D)\, dD, \tag{5}$$

where N_{RO} and Λ are constants. N_{RO} and Λ may be related to N_R, the total concentration of raindrops, by

$$N_R = \int_0^\infty N_{RO} \exp(-\Lambda D)\, dD = N_{RO}/\Lambda, \tag{6a}$$

and to Q_R by

$$Q_R = (1/\rho_a \int_0^\infty (4/3)\pi \rho_w (D/2)^3 N_{RO} \exp(-D) dD = \pi (\rho_W/\rho_a) N_{RO} \Lambda^{-4}; \tag{6b}$$

solving (6a) and (6b), we obtain

$$N_{RO} = (\pi \rho_W/\rho_a Q_R)^{1/3} N_R^{4/3}, \tag{7a}$$

and

$$\Lambda = N_{RO}/N_R = (\pi N_R \rho_W/\rho_a Q_R)^{1/3}. \tag{7b}$$

The mean raindrop radius, R_R, is then defined in terms N_{RO} and Λ as the average surface area-weighted radius, i.e.,

$$R_R = \left[\int_0^\infty (D/2)^2 N_{RO} \exp(-\Lambda D)\, dD/N_R\right]^{1/2} = 1/(\sqrt{2}\Lambda) = \left(\frac{\rho_a Q_R}{\sqrt{8}\,\pi \rho_W N_R}\right)^{1/3}. \tag{8}$$

Similarly, U in (1) is defined as the mass-weighted, average fall velocity; using Liu and Orville's (1969) formula for the fall velocity of a single raindrop, we obtain

$$U = 1845\,(\rho_a\, Q_R/\rho_W\, N_R)^{0.267}, \tag{9}$$

in units of m/s.

Having defined N_c, R_c, N_R, R_R, and U, values for CONDC, CONDR, and COLL can be represented with relatively simple formulae. For instance, the rate of condensation to cloudwater can be written as (Schwartz, 1983)

$$\text{CONDC} = 4\pi D_W\, N_c \frac{R_c}{1 + \dfrac{4l}{3R_c\,\alpha}}\,(Q_V - Q_{VS}), \tag{10}$$

where D_W is the molecular diffusion coefficient for water (see Fig. 1), l is the mean free path taken here to be 10^{-7} m, and α is the sticking coefficient, which similar to Chameides (1984) is assumed to be 10^{-2}. The rate of condensation to rainwater, CONDR, is similar to (10) except that because $R_R \ll R_c$, the term involving α may be dropped and, to account for increased condensation due to convective and turbulent enhancements in the rate of transport of material to the surface of a large drop, a ventilation factor, $f(R_R)$, must be added. Hence

$$\text{CONDR} = 4\pi D_W\, N_R\, R_R f(R_R)\,(Q_V - Q_{VS}), \tag{11}$$

where $f(R_R)$ is given by Frossling's equation

$$f(R_R) = 1 + 0.23\,(2R_R\, U/\nu)^{0.5}, \tag{12}$$

and ν, the kinematic viscosity of air, is equal to 1.65×10^{-5} m^2/s.

The conversion of cloudwater to rainwater is parameterized in terms of two processes: autoconversion and collision coalescence. Autoconversion, representing the process by which cloud droplets grow to sizes large enough to be considered small raindrops, tends to be most important in the early stages of cloud development. Collision and coalescence on the other hand, which involves the growth of pre-existing raindrops by collecting smaller cloud droplets, dominates in the later stages of the cloud. In our calculations we adopt the formula-allowing for the conversion of cloudwater to autoconversion. In this formulation, the rate of autoconversion is specified to be equal to zero until the value of a "trigger function", $F(z,t)$ is equal to or greater than 1. Whenever $F(z,t) \geqslant 1$, the autoconversion rate is taken to be proportional to Q_c^2. Hence

$$\text{AUTO} = \begin{cases} 0 & \text{for } F(z,t) < 1 \\ \dfrac{J\rho_a\, Q_c^2}{60}\left(6 + \dfrac{0.02\, N_c}{D_c\,\rho_a\, Q_c}\right)^{-1} & \text{for } F(z,t) \geqslant 1, \end{cases} \tag{13}$$

where D_c is a constant related to the relative dispersion of the cloud droplet size distribution, J is a normalization factor, and $F(z,t)$ is obtained from the solution to differential equation (14)

$$\frac{\partial F}{\partial t} = -W\frac{\partial F}{\partial t} + K\frac{\partial^2 F}{\partial z^2} + \frac{\rho Q_c}{60}\left(2 + \frac{0.02\, N_c}{D_c\,\rho Q_c}\right)^{-1}. \tag{14}$$

In our Standard Model, N_c/D_c was assumed to be 400, a ratio appropriate for maritime conditions and J was taken to be 0.25, the value Hu et al. found gave the closest fit to observations.

Note that in as much as the autoconversion rate is taken to depend upon Q_c to the second power, the above formulation is similar to the parameterizations of Berry (1968) and Simpson and Wiggert (1969). However unlike these other parameterizations, a trigger function is used to delay the onset of the autoconversion process. As will be illustrated later, by tying the onset of autoconversion to this trigger function, the initial formation of raindrops does not begin until roughly one hour has elapsed. Furthermore, once it has begun, rain formation by autoconversion is largely limited to the middle and upper levels of the cloud. Both these effects slow the rate of autoconversion and thereby alleviate the problem common to other parameterized models of developing in-cloud rainwater too rapidly (c.f. Silverman and Glass, 1973).

Using a continuous model for collision and coalescence, the rate of conversion of cloudwater to rainwater can be represented by (15)

$$\text{COLL} = \int_0^\infty N_{ro} \exp(-\Lambda D)\,\pi\,(D/2)^2\, UEQ_c\, dD, \tag{15}$$

Table 1. *Cloud physics parameters and results*

	Model			
	Standard Model	Model 1	Model 2	Model 3
Input parameters				
W (m/s)	0.1	0.05	0.1	0.1
K (m²/s)	20	20	40	20
J	0.25	0.25	0.25	0.50
Results				
time of initial rain (min)	60	100	60	60
maximum rain intensity (mm/h)	4.6	2.5	4.6	4.5
time of maximum rain (min)	100	130	90	100
steady state rain intensity	2.4	1.1	2.3	2.5
average total steady state liquid water concentration ($Q_R + Q_C$ (g/kg)	0.46	0.32	0.45	0.45

where E is the mean collision-coalescence efficiency and is taken to be 0.8 in our calculations. Substituting for N_{RO} and Λ, we obtain (16) for COLL.

$$\text{COLL} = 9035\,(\rho_W/\rho_a\,Q_R)^{-0.933}\,N_R^{0.067}\,EQ_c. \qquad (16)$$

The solutions for Q_V, Q_R, and Q_C were obtained by integrating (1) subject to the following initial and boundary conditions. At time $t = 0$, water vapor was assumed to be saturated (i.e., $Q_V(z,0) = Q_{VS}$) while all liquid water was assumed to be absent (i.e., $Q_C(z,0) = Q_R(z,0) = 0$). A nominal cloud depth of 3 km was obtained by applying the boundary conditions of zero cloudwater at $z = 0$ and $z = 3$ km, as well as zero rainwater at $z = 3$ km. In addition, a zero vertical gradient condition was applied to Q_R at $z = 0$ km. In all cases, W was assumed to be constant in time and space. The values adopted for W and other important parameters are listed in Table 1 along with the key results of the model simulations.

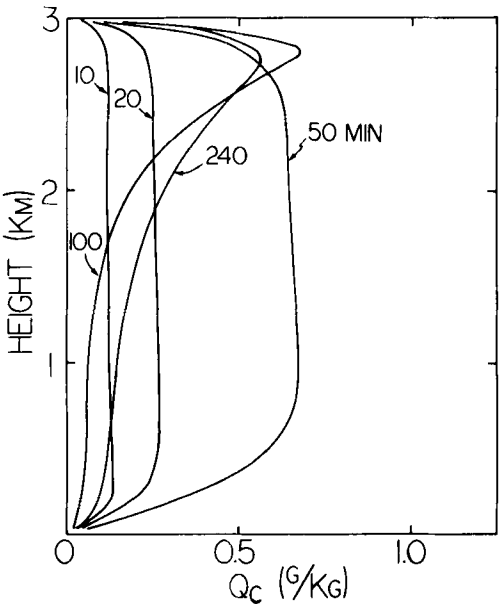

Fig. 2. The calculated cloudwater mixing ratio, Q_C, as a function of height above the cloudbase in the Standard Model for $t = 10$, 20, 50, 100, and 240 min.

2.2. *Physical model results*

In the Standard Model, an updraft velocity of 0.1 m/s was assumed. The resulting profiles of cloudwater, $\bar{Q}_C$, and rainwater $\bar{Q}_R$, as well as the trigger function, F, are presented in Figs. 2, 3, and 4, respectively. During the first hour we find a rapid rise in cloudwater levels but, because $F < 1$ at all levels no rainwater is produced. At about 60 min, however, F reaches a value of 1 (see Fig. 4) and the autoconversion of cloudwater to rainwater begins. After this time there is a rapid rise in rainwater and decrease in cloudwater as rain drops are initially produced in the middle and upper levels of the cloud by autoconversion and then grow by collision and coalescence as they fall through the cloud. The highest levels of cloudwater are generally found in the upper levels of the cloud while those of rainwater are found near the cloudbase; this dependence of Q_R and Q_C upon z is indicative of the importance of the

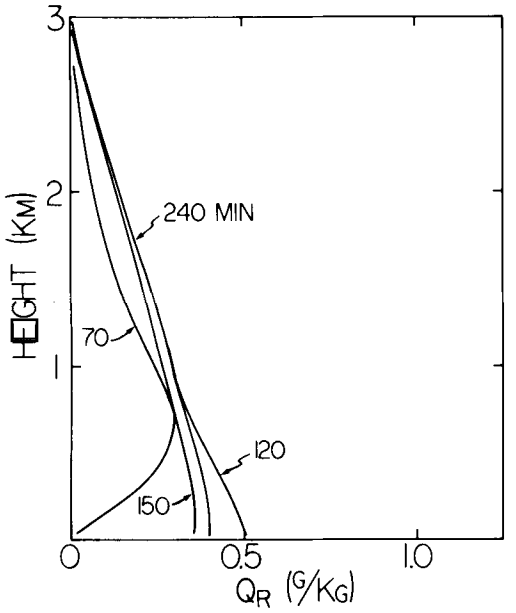

Fig. 3. The calculated rainwater mixing ratio as a function of height above the cloudbase in the Standard Model for $t = 70$, 120, 150, and 240 min.

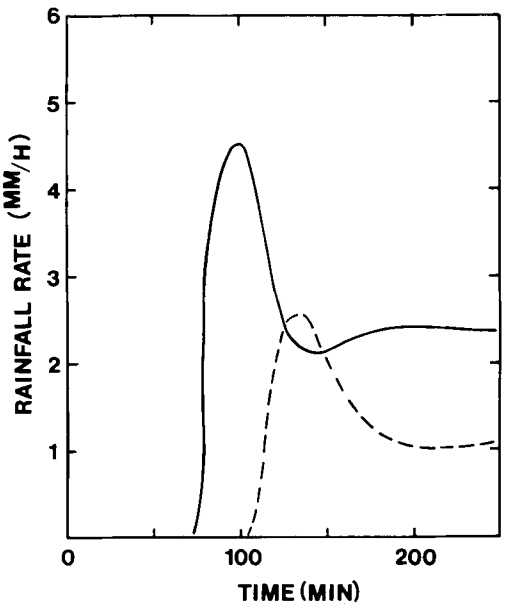

Fig. 5. The calculated rainfall rate as a function of time for the Standard Model (solid line) and for Model 1 with $W = 0.05$ m/s (dashed line).

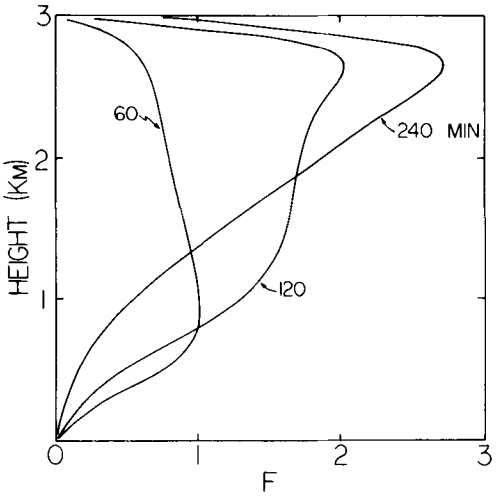

Fig. 4. The calculated values for the trigger function, F, as a function of height above the cloudbase in the Standard Model for $t = 60$, 120, and 240 min.

collision and coalescence process in controlling the rate of production of rainwater.

In Fig. 5, the calculated rainfall rate (defined here as the rate at which rainwater falls out of the cloud due to sedimentation) is illustrated as a function of time. We find that precipitation begins soon after the autoconversion process begins and rapidly increases to a maximum value of about 4.5 mm/h after about 100 mins in the Standard Model case. Following this maximum, the rainfall rate decreases and eventually reaches a fairly constant value of about 2 mm/h after 180 mins. This constant rainfall rate of 2 mm/h is balanced by an equivalent flux of water vapor into the cloud by advection and eddy diffusion. In fact after about 180 min, the whole cloud system tends to a steady state with fairly constant distributions of liquid water as well as rainfall. In the model calculations this steady state continues essentially ad infinitum, because we have assumed a constant updraft velocity as well as constant boundary conditions. In the real atmosphere the conditions of high humidity and upward motion that cause the formation of the cloud would eventually change and the cloud and its attendant precipitation would cease. In a similar vein we could easily simulate the end of the precipitation in the model by either allowing W to go to zero or reducing the assumed bottom

boundary condition on Q_V after some specified period of time.

The cloud model contains a number of adjustable parameters whose values can potentially affect the results. The sensitivity of the calculations to variations in three of these parameters — namely, W, the updraft velocity, K, the eddy diffusion coefficient, and J, the trigger function's normalization factor — have been explored in Models 1, 2, and 3. A description of these models and the key results from them are presented in Table 1. We find that Models 2 and 3, in which K and J were varied, yield results basically equivalent to that of the Standard Model; rainfall in all of these cases starts after about 60 min, the maximum rainfall rate is about 4.5 mm/h, and the steady state rainfall rate is approximately 2 mm/h. By contrast, Model 2 in which W was changed from 0.1 m/s to 0.05 m/s is significantly different from that of the Standard Model; rainfall in Model 2 starts after about 100 min as opposed to 60 min and the maximum and steady state rainfall rates are reduced by almost a factor of two (see Fig. 5).

The model described above appears to capture many of the key elements of a warm stratiform cloud. The calculated cloudwater and rainwater concentrations are reasonably close to those typically found in clouds of this category, as are the calculated rainfall rates (c.f. Pruppacher and Klett, 1978). Furthermore the strong sensitivity of the model to the updraft velocity is also reflected in the atmosphere where larger updraft velocities generally lead to more intense precipitation. Having described the cloud physics model, we now discuss the application of this model to the problem of the removal of soluble gases from the atmosphere.

3. Simulating an inert soluble tracer

A soluble trace species can be present in a cloud in three forms: as a gas, as a dissolved constituent of the cloudwater, and as a dissolved constituent in the rainwater. We use $G(I)$ to represent the volume gas-phase mixing ratio (i.e. v/v) of species I. Similarly $C(I)$ and $R(I)$ are used to represent the equivalent volume mixing ratios of I in cloudwater and rainwater, respectively. As in Chameides (1984), the equivalent mixing ratio of a dissolved species is the gas-phase mixing ratio this species would attain if it were completely transferred from the aqueous phase to the gas phase. Thus if $[I]_C$ is the concentration in M (i.e. moles/liter) of I in cloudwater, then $C(I)$ is given by

$$C(I) = [I]_C\,(Q_C \times \rho_a \times 10^{-3})\,(6.02 \times 10^{23})/n_M, \tag{17}$$

where n_M is the total atmospheric number density. Similarly,

$$R(I) = [I]_R\,(Q_R \times \rho_a \times 10^{-3})\,(6.02 \times 10^{23})/n_M, \tag{18}$$

where $[I]_R$ is the concentration of I in rainwater.

Similar to that of water vapor, the three continuity equations governing the time rate of change in species I in a cloud are given by (19)

$$\partial G(I)/\partial t = -W\,\partial G(I)/\partial z - \mathrm{SCAVC} - \mathrm{SCAVR} + K\,\partial^2 G(I)/\partial z^2, \tag{19a}$$

$$\partial C(I)/\partial t = -W\,\partial C(I)/\partial z + \mathrm{SCAVC} - (\mathrm{COLL}) \times (\mathrm{C(I)/Q_C}) - (\mathrm{AUTO}) \times (C(I)/Q_C) + K\,\partial^2 C(I)/\partial z^2, \tag{19b}$$

$$\partial R(I)/\partial t = -(W-U)\,\partial R(I)/\partial z + \mathrm{SCAVR} + (\mathrm{COLL}) \times (\mathrm{C(I)/Q_C}) + \mathrm{AUTO} \times (C(I)/Q_C^2) + K\,\partial^2 R(I)/\partial z^2, \tag{19c}$$

where AUTO and COLL are as given above and SCAVC and SCAVR represent the rate of scavenging of I from the gas phase to cloudwater and rainwater, respectively. Similar to the expressions for the condensation of water vapor, the scavenging rates are given by (20)

$$\mathrm{SCAVC} = 4\pi\,D_1\,N_C\,\frac{R_C}{1 + 4l/3R_C\,\alpha}\left(G(I) - \frac{[I]_C\,p}{H_C(I)}\right), \tag{20a}$$

$$\mathrm{SCAVR} = 4\pi\,D_1\,N_R f(R_R)\,R_R\left(G(I) - \frac{[I]_R\,p}{H_R(I)}\right) \tag{20b}$$

where p is the pressure in atmospheres, D_1 is the molecular diffusion coefficient of I and for simplicity is assumed to be the same as that for water vapor, and $H_C(I)$ and $H_R(I)$ are the effective solubility constants for species I in cloudwater and rainwater, respectively. Note that a species' effective solubility constant differs

from the standard solubility constant in that it takes into account the effects of dissociation and complex formation upon the species' net solubility. Because the degree of dissociation and complex formation of a species depends upon the properties of the solution (i.e., pH) and because the properties of cloudwater and rainwater change as a function of time and space, H_c and H_R can also vary with time and space. Furthermore since the composition of cloudwater and rainwater within a given cloud can be different, H_c and H_R are not necessarily equal. However, in the calculations presented here we will ignore these effects and simply let $H_c = H_R = H$, where H is independent of t and z. To study the effects of varying solubility on the removal rate of a species from clouds, we have carried out calculations for H varying from 10^3 M/atm, which would correspond to a relatively insoluble species, to 10^{11} M/atm, which would correspond to an extremely soluble species such as HNO_3.

In order to solve (19), initial conditions as well as boundary conditions are needed. For simplicity, we assume species I to be well-mixed in the cloud-free atmosphere with a constant ambient concentration, $G(I)_0$, of 25 pptv, and thus the initial gas-phase mixing ratio for the species was taken to be 25 pptv. Since all our results scale linearly with the assumed ambient concentration of I, extending the calculations presented here to species with other ambient concentrations is easily accomplished. The initial values for $C(I)$ and $R(I)$ were set equal to zero. Boundary conditions for $G(I)$, $C(I)$, and $R(I)$ were similar to those adopted for the equivalent water vapor and liquid water mixing ratios. $G(I)$ at $z = 0$ km and 3 km was held fixed at the assumed ambient level of 25 pptv. $C(I)$ at both 0 and 3 km was set equal to zero as was $R(I)$ at 3 km. Similar to that used for Q_R, a zero gradient condition was adopted for $R(I)$ at the cloudbase.

4. Gas- and aqueous-phase distributions

The calculated variations in $G(I)$, $C(I)$, and $R(I)$ as a function of altitude for various selected times are illustrated in Fig. 6, 7 for $H = 10^3$ and 10^7 M/atm, respectively. In the case of $H = 10^3$ M/atm, which corresponds to a sparingly soluble species, the presence of the cloud has only a

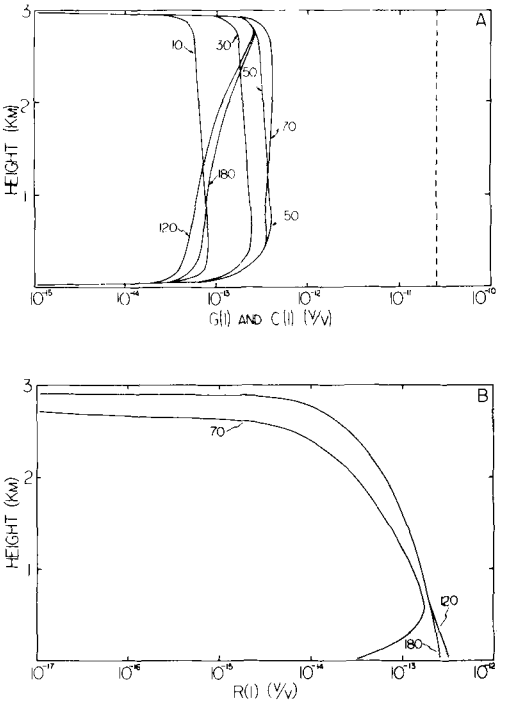

Fig. 6. The calculated in-cloud concentrations of a species with $H = 10^3$ M/atm as a function of height above the cloudbase at various times during the simulation. The gas-phase mixing ratio, $G(I)$ is shown by the dashed line in *A* and remains essentially unchanged throughout the calculation. The equivalent mixing ratio in cloudwater, $G(I)$, is shown by the solid lines in *A*. The equivalent mixing ratio in rainwater, $R(I)$, is shown in *B*.

negligible effect upon the species' gas-phase concentration. Thus note in Fig. 6 that $G(I)$ remains essentially unchanged throughout the calculation and a very small fraction of the species' total mass is transferred to the aqueous phase. Equilibration between the gas and aqueous phases occurs in less than a minute (Chameides, 1984) and thus the changes in $C(I)$ and $R(I)$ as a function of time that are apparent in Figure 6A and 6B are essentially caused by changes in the total concentration of cloud- and rainwater (see Figs. 3 and 4).

In contrast to the case of $H = 10^3$ M/atm, clouds have a major impact upon the species' distribution when $H = 10^7$ M/atm. As illustrated in Fig. 7, we find that within a few minutes virtually all of the species is transferred from the

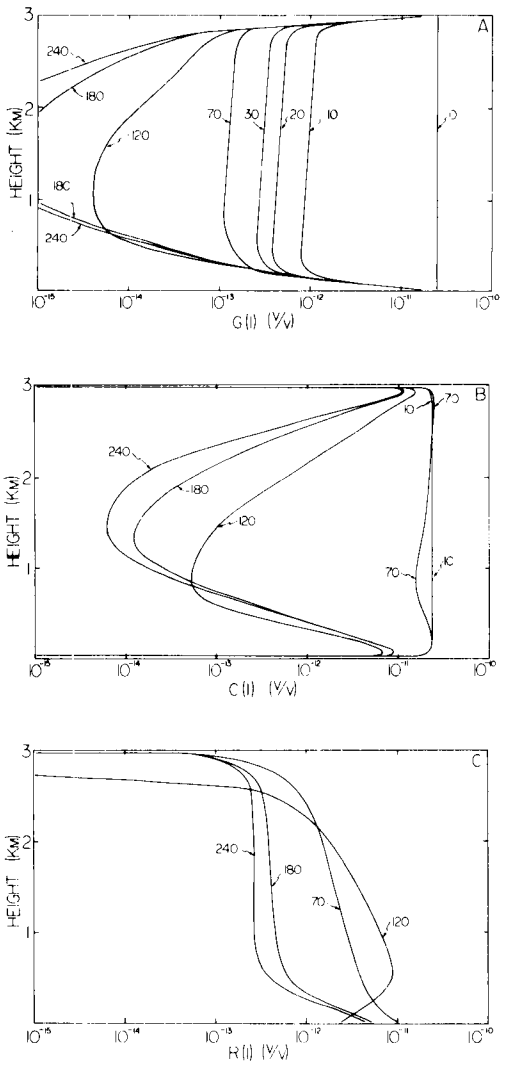

Fig. 7. The calculated in-cloud concentrations of a species with $H = 10^7$ M/atm as a function of height above the cloudbase at various times during the simulation. The gas-phase mixing ratio, $G(I)$ is shown in A, the equivalent mixing ratio in cloudwater, $C(I)$, is shown in B, and the equivalent mixing ratio in rainwater, $R(I)$, is shown in C.

gas phase to the cloudwater. Except near the very top and bottom of the cloud where the transport of material into and out of the cloud by advective and eddy diffusive-fluxes have a significant effect, $G(I)$ rapidly falls to negligibly small levels while $C(I)$ rises to a value essentially equal to the outside ambient level of 25 pptv. $C(I)$ remains at this level until about 1 h has elapsed and rainwater begins to form. As rainwater levels increase due to autoconversion and collision and coalescence, $C(I)$ decreases. During the initial stages of rainwater formation the decrease in $C(I)$ is matched by a corresponding increase in $R(I)$. Eventually, however, as raindrops containing significant quantities of I as a solute fall out of the cloud, species I becomes depleted inside the cloud and $R(I)$ as well as $C(I)$ decreases. The depletion continues until t is about 150 min and the total concentration of I near the center of the cloud has fallen to less than 0.3 pptv. At this time an approximate steady state is reached with $G(I)$, $C(I)$, and $R(I)$ maintaining fairly constant values. Similar to the steady state that is reached with water, the steady state in the concentrations in species I reflects a balance between the influx of I as a gas at the top and bottom of the cloud and the loss of I from the cloud in rainwater falling through the cloudbase. The details of this balance will be described in more detail in the next section.

It is of interest to identify the processes that control the steady state levels of species I in rainwater. Recall from (19c) that the time rate of change in $R(I)$ is determined by five basic processes. These are: (1) the source of $R(I)$ from the direct scavenging of gaseous I; (2) the source of I from the autoconversion of cloudwater already containing I; (3) the source of I from the collection of cloudwater by collision and coalescence; (4) the vertical flux divergence of $R(I)$ from sedimentation and advection of rainwater; (5) the flux divergence of $R(I)$ from eddy diffusion. The calculated values of each of these terms as a function of altitude are illustrated in Fig. 8 for a representative value of H (i.e., 10^5 M/atm) and $t = 200$ min. It is apparent from this figure that the two dominant terms are the source of dissolved I in rainwater due to collision and coalescence of cloudwater and the loss of $R(I)$ that arises from sedimentation of the raindrops. In the lower portion of the cloud, however, where cloudwater concentration are small and the concentration of gaseous I is largest, scavenging supersedes collision and coalescence as the major source of I to the rainwater. Thus throughout most of the cloud the flow of species I is from the gas phase to cloudwater and then to rainwater via

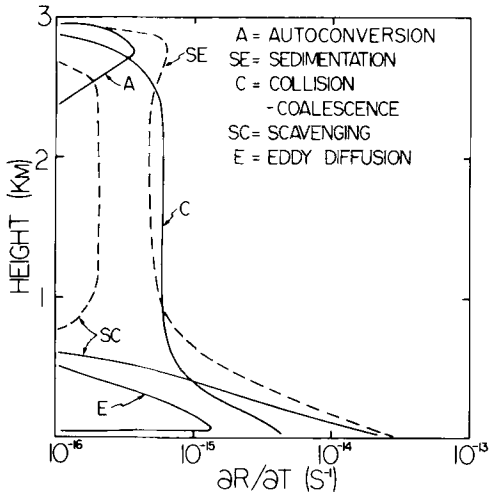

Fig. 8. The calculated rates of change in $R(I)$ as a function of height above the cloudbase due to autoconversion of cloudwater to rainwater, the sedimentation of rainwater, the conversion of cloudwater to rainwater by collision and coalescence, the direct scavenging of gaseous I by raindrops, and the transport of rainwater by eddy diffusion. Terms causing a positive change in $R(I)$, (i.e., $dR/dt > 0$) are indicated by a solid line and terms causing a negative change in $R(I)$ (i.e. $dR/dt < 0$) are indicated by a dashed line. The results shown are for $H = 10^5$ M/atm and $t = 200$ min.

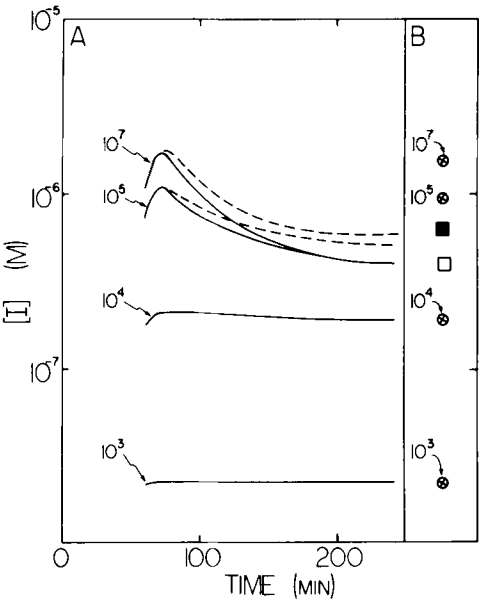

Fig. 9. The calculated concentration (in moles/liter) of species I dissolved in rainwater falling through the cloudbase for various values of the solubility constant, H. In A, the model-calculated concentrations are shown for the Standard Model (solid line) and for Model 2 with K doubled to a value of 40 m²/s (dashed line). In B the concentrations calculated from formula (24) are shown by the circled X's and those calculated from (31) are shown by squares. The open square is for $K = 20$ m²/s and the closed square is for $K = 40$ m²/s.

collection of cloud droplets; it is only at the very lowest layers of the cloud that species I flows directly from the gas phase to the raindrops by scavenging.

5. Removal rates

Having established how soluble species are apportioned among the gas phase and liquid phases of a stratiform cloud, we now turn to the rates at which these species are removed from the cloud via rainout. In Fig. 9 the calculated values of $[I]_{R,z=0}$, the concentration of species I in the rainwater falling through the cloudbase and out of the cloud, is plotted as a function of time for $H = 10^3$, 10^4, 10^5, and 10^7 M/atm and for $K = 20$ and 40 m²/s. The results for $H > 10^7$ M/atm are not shown as they are indistinguishable from those obtained with $H = 10^7$ M/atm. Two basic patterns for the variations of $[I]_{R,z=0}$ with time and solubility are apparent in Fig. 9. For low solubility species (i.e., $H < 10^5$ M/atm), $[I]_{R,z=0}$ varies approximately linearly with H but is independent of time, while for high solubility (i.e., $H > 10^5$ M/atm) $[I]_{R,z=0}$ varies with time but does not depend upon H.

The temporal variations in $[I]_{R,z=0}$ generally follow those of $R(I)$. For the cases of low solubility, recall that the gas- and aqueous-phase mixing ratios were found to be essentially constant in both time and space after an initial brief induction period during the very early stages of cloud development. As a result the concentration of I in the rainwater falling out of the cloud is also found to be essentially constant in time when the solubility is low. The much more complex pattern for $[I]_{R,z=0}$ in the high solubility cases is indicative of the large temporal variations obtained for $R(I)$. Thus similar to the results in Fig. 7c, $[I]_{R,z=0}$ in these cases reaches a maximum value soon after the onset of precipitation, then

decreases and eventually reaches a fairly constant value towards the end of the calculation. It is interesting to note that this model-calculated trend in $[I]_{R,z=0}$ is qualititatively consistent with observations in that sequential sampling and analysis of rainwater reaching the earth's surface during a single storm generally reveals a similar trend in the concentrations of highly soluble species and particles (c.f., Dingle and Gatz, 1966; Kins, 1982; Zika et al., 1982).

The dependence of $[I]_{R,z=0}$ upon the solubility constant, H, can be understood by considering a simple box model in which liquid water drops with a mass mixing ratio of Q_W are introduced into a parcel of air containing species I as a gas with a concentration of $G(I)_0$. According to Henry's Law, when thermodynamic equilibrium between the gas and aqueous phases is attained. $[I]_{eq}$, the equilibrium aqueous-phase concentration of species I, is related to its equilibrium gas-phase mixing ratio, $G(I)_{eq}$, by

$$[I]_{eq} = H\,p\,G(I)_{eq}. \tag{21}$$

Furthermore mass balance requres that

$$G(I)_o = G(I)_{eq} + [I]_{eq}\,Q_W\,\rho_a\,A \times 10^{-3}/n_M, \tag{22}$$

where n_M is the total atmospheric number density. Combining (22) and (23) we obtain an expression for the equilibrium concentrations of I in terms of its ambient concentration, its solubility, and the total liquid water content, i.e.,

$$G(I)_{eq} = G(I)_0/(1 + H\,p\,Q_W\,m_a \times 10^{-3}), \tag{23}$$

$$[I]_{eq} = G(I)_0)1/(Hp) + Q_w m_a \times 10^{-3}), \tag{24}$$

where m_a is the mean molecular weight of air. Adopting a value for $G(I)_0$ of 25 pptv and Q_W of 0.55 g/m^3 (i.e. 0.46 g/kg), equal to the average total liquid water content of the Standard Model (see Table 1), (24) was solved as a function of H and the resulting values for $[I]_{eq}$ are illustrated in Fig. 9.

Note in Fig. 9 that, like the model calculated values for $[I]_{R,z=0}$, $[I]_{eq}$ is predicted by (24) to vary linearly with H for low solubility and be independent of H for high solubility. For species with low solubility such that

$$H\,p\,Q_W\,m_a \times 10^{-3} \ll 1, \tag{25}$$

only a minor fraction of the species' mass resides in the aqueous phase. In this case (24) reduces to

$$[I]_{eq} = G(I)_{eq}\,H\,p = G(I)_o\,H \tag{26}$$

and the concentration in the condensed phase is linearly related to H. On the other hand, in the case of high solubility such that

$$H\,p\,Q_W\,m_a \times 10 \gg 1, \tag{27}$$

virtually all of the species resides in the condensed phase so that

$$[I]_{eq} = G(I)_0/(Q_W\,m_a \times 10^{-3}) \tag{28}$$

and $[I]$ becomes independent of H.

Comparing the concentration of I predicted from (24) with the more complete model results in Fig. 9 indicates excellent quantitative agreement for the low solubility cases but significant differences for high solubility. In the later case, the values predicted from (24) agree well with the model at the onset of the precipitation when $[I]_{R,z=0}$ is a maximum but overestimates the concentrations thereafter.

In order to understand why (24) overestimates the concentration of highly soluble species in rainwater it is useful to first consider the sources and sinks of I to and from the cloud. The major sources of I to the cloud include the upward advective flux of gaseous I through the cloudbase due to advection as well as the eddy-diffusive fluxes of gaseous I through the top and bottom of the cloud. These sources can be approximated by $S(I)$ in (29)

$$S(I) \approx G(I)_o\,n_M\,[W + 2(K/\Delta z)], \tag{29}$$

where S is in units of molecules cm^{-2} s^{-1} and Δz represents the scale height for gaseous I within the cloud. In (29) the first term on the right-hand side represents the source of I due to advection from below and the second term represents the sources from above and below due to turbulent diffusion (assumed for simplicity to be equal). The major sinks are the upward advective flux of I through the cloud top and the loss due to rainout. This later term can be related to $[I]_{R,z=0}$ by

$$L(I) = [I]_{R,z=0}\,Q_R(U - W) \times \rho_a \times 10^{-3} \times 6.02 \times 10^{23}, \tag{30}$$

where $L(I)$ is the rate of loss of I from the cloud in units of molecules cm^{-2} s^{-1}.

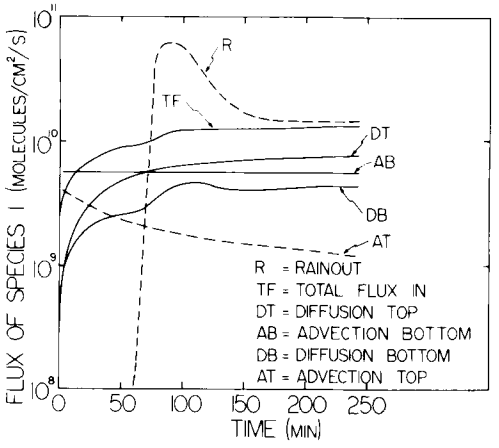

Fig. 10. The fluxes of species I into and out of the cloud as a function of time due to rainout, eddy diffusion through the top and bottom of the cloud, and advection through the top and bottom of the cloud. Fluxes into the cloud are indicated by solid lines and fluxes out of the cloud are indicated by dashed lines.

In Fig. 10, the calculated values for each of the sources and sinks of I are plotted as a function of time for an illustrative case (i.e., $H = 10^5$ M/atm). Similar to the variations in $[I]_{R,z=0}$, $L(I)$ reaches a maximum value soon after the onset of precipitation. However, note in Fig. 10 that for this high a value of $L(I)$, the rate of loss of species I from the cloud is much greater than the rate at which I is supplied to the cloud by advection and turbulent transport. As a result, both the abundance of I and the concentration of I in the rain leaving the cloud decrease (as in Fig. 7, 9). This downward trend in the in-cloud abundance of I causes a corresponding decrease in $L(I)$; however, because a decrease in the concentration of I in the cloud cause an increase in the vertical gradient of $G(I)$ at the cloud boundaries, the downward trend also has the effect of increasing the source of I to the cloud by eddy transport (see Fig. 10). This trend continues until t is about 150 mins when, as illustrated in Fig. 10, an order of magnitude balance between the loss and source of I is attained (i.e., $L(I) \approx S(I)$) and the approximate steady state described previously is established.

Thus in order to establish the steady state for a highly soluble species it is first necessary for the total abundance of the species in the cloud to fall well-below its ambient level. It is therefore not surprising that (24) overestimates the concentration of I in the rainwater leaving the cloud since a key assumption in deriving this equation was that the total abundance of I in the cloud is always given by $G(I)_0$ (see for instance (22)). Because highly soluble species become depleted in the cloud, thereby causing the rate of removal to fall below that predicted by (24), care must be taken when trying to simulate rainout in photochemical models with simple first-order parameterizations. As noted by previous investigators (Rodhe and Grandell, 1981; Thompson and Cicerone, 1982; Stewart et al., 1983; Giorgi and Chameides, 1984) it is imperative that these parameterizations include corrective terms to account for the effects of transient processes such as the one apparent in Fig. 9.

Since the rate of removal of highly soluble species appears to be essentially controlled by the rate at which new material is supplied to the cloud by transport, a more accurate expression than (24) for the concentration of I in the rainwater leaving the cloud in this case can be obtained by demanding that $L(I) = S(I)$ and solving for $[I]_{R,z=0}$ from (29) and (30). The resulting expression is given by (31)

$$[I]_{R,z=0} = G(I)_0(W + 2(K/\Delta z))/Q_R(U - W) \times m_a \times 10^{-3}). \quad (31)$$

That this equation more accurately predicts the concentration of I for highly soluble species is evident in Fig. 9 where the values for $[I]_{R,z=0}$ calculated from (31) is illustrated. In solving (31), we assumed a value of 200 m for Δz based upon the results in Fig. 7.

Thus our calculations imply that the rate of rainout is controlled by a combination of thermodynamics and transport. For low solubility species, the rate of removal is controlled by a simple thermodynamic partitioning of the ambient air between the gas and aqueous phases of the cloud. In this case, the removal rate is relatively slow and transport of the gas into the cloud from the outside air is fast enough to always maintain the species' concentration within the cloud at its ambient level. For high solubility species a more complex situation arises with the removal rate being transport limited. In this case virtually all of the species resides in the

aqueous phase and the rate of removal is quite rapid. Given this rapid rate of removal, transport processes cannot transfer gas from the outside air to the cloud fast enough to maintain the concentration of I in the cloud at its ambient level. As a result the species becomes depleted and the rate of removal via rainout slows until it is equal to the rate at which transport can transfer new material to the cloud from the outside air. Thus in the case of highly soluble species the rate of rainout removal is controlled by transport rather than by thermodynamics.

In the light of the above conclusion it is interesting to note that turbulent transport appears to be a dominant source of highly soluble gases to stratiform clouds. For example note in Fig. 10 that eddy diffusion transfers about twice as much material into the cloud as does advection due to the updraft; the sources due to advection at the cloudbase, eddy diffusion at the cloudbase, and eddy diffusion at the cloud top are all approximately equal. As a result changing the eddy diffusion coefficient can have a significant effect upon the calculated removal rate of highly soluble species. Note for instance in Fig. 9 that doubling K from 20 to 40 m^2/s caused $[I]_{R,z=0}$ to increase by about 50% for highly soluble species. (Increasing K has no effect for low solubility species because in these cases no significant vertical gradients in $G(I)$ are established and as a result eddy diffusion is not important.) Thus while turbulence is a poorly understood process which can only be treated in models with highly simplified parameterizations, our calculations imply that this process plays a major role in controlling the rate at which highly soluble species are removed from the atmosphere by rainout from stratiform clouds. In order to better understand the rainout process and its variability during a single storm as well as from storm to storm, it would appear therefore that further work is needed on turbulence and its role in transporting material into and out of stratiform clouds.

6. Conclusion

Model calculations indicate that the removal of soluble species from warm stratiform clouds is accomplished by first dissolving the species in cloudwater, then transferring the dissolved material to raindrops when the cloudwater is converted to rainwater by collision and coalescence, and finally removing the species from the cloud in the raindrops as they fall through the cloudbase. For sparingly soluble species, only a small fraction of the species' total mass is dissolved in cloud- and rainwater and as a result the rate of removal is accurately described in terms of a simple partitioning of the ambient air between the gas and aqueous phases. For highly soluble species, on the other hand, virtually all of the species' mass within the cloud is transferred to the condensed phase. As the rainwater falls out of the cloud in this case, the species' abundance in the cloud is depleted and the rate at which the species is removed from the cloud is slowed. The rate of removal continues to slow until a balance is reached between this loss and the rate at which new gas is transported into the cloud; at this point an approximate steady state is attained in the cloud with the concentration of the species and its rate of removal remaining essentially constant. For the Standard Model about 150 minutes was required for this steady state to be established.

While the model-calculated concentration of a sparingly soluble species in the rainwater is predicted to be fairly constant in time for a given constant updraft velocity, the concentration of a highly soluble species is found to reach a maximum soon after the onset of precipitation, then decrease as the storm proceeds, and finally reach a constant value as the balance between source and loss described above is attained. Similar trends are generally observed in rainwater collected at the earth's surface during a single storm.

An interesting facet of our calculations is the fact that turbulent transport is found to be a major source of highly soluble gases to stratiform clouds. This result has a number of potentially important implications for the study of cloud and precipitation chemistry. For one, because the simulation of turbulent transport is highly parameterized, the model-calculated removal rate of a highly soluble species from a given cloud is subject to a fairly significant uncertainty and thus a quantitative comparison of the model results with observations from a single event is problematic. Furthermore because turbulent processes are likely to be highly variable in time and space, we

might expect the rate of removal of a highly soluble species to vary considerably even when other parameters such as the precipitation rate and the species' ambient concentration do not vary. In addition some caution needs to be exercised in interpreting observations of the concentrations of trace species within and outside of stratiform clouds; for instance, because turbulent transport does not represent a significant source of sparingly soluble species to clouds, the ratio of the total abundance of a highly soluble species (i.e. HNO_3) to that of a relatively insoluble species (i.e., NO_2) will not necessarily be the same as the equivalent clear-air ratio even in the case of a non-precipitating cloud.

Finally, it should be noted that the model calculations presented here have neglected two potentially important processes, that is the below-cloud evaporation of raindrops and the scavenging of soluble gases below the cloud as the drops falls towards the earth's surface. The evaporation of rainwater below the cloud will have the obvious effect of lowering the rate at which a species is removed from the atmosphere, although the magnitude of this effect will depend on the species' concentration below the cloud as well as the species' solubility. While below-cloud scavenging (i.e. washout) will enhance the total rate of removal of a soluble species from the atmosphere, it may lower the rate of removal via rainout since the depletion of a species' concentration below the cloud by washout will lower the rate at which advection and turbulence can transport new gas through the cloudbase and into the cloud. Model calculations simulating these below-cloud effects as well as the in-cloud processes simulated in the model described here are needed to better understand the rate of removal of soluble species from the atmosphere by the two coupled mechanisms of rainout and washout.

7. Acknowledgements

This work was supported in part by funds from the National Aeronautics and Space Administration under Grant NAG-1-85 and from the National Science Foundation under Grant ATM-8208828.

REFERENCES

Berry, E. X. 1968. Modification of the warm rain process, Proc. First Nat. Conf. on Weather Modification. *Amer. Meteorol. Soc.*, Albany, New York.

Best, A. C. 1952. Effect of turbulence and condensation on drop-size distribution in cloud. *Q. J. R Meteorol. Soc. 78*, 28–36.

Chameides, W. L. and Davis, D. D. 1982. Chemistry in the troposphere. *Spec. Rep Chem. Eng. News. 60*, 38–52.

Chameides, W. L. 1984. Photochemistry of a remote marine stratiform cloud. *J. Geophys. Res. 89*, 4739–4755.

Brimblecome, P. and Dawson, G. A. 1984. Wet removal of highly soluble gases. *J. Atmos. Chem. 2*, 95–107.

Dingle, A. F. and Gatz, D. F. 1966. Air cleansing by convective rains. *J. Appl. Meteorol. 5*, 160–168.

Giorgi, F. and Chameides, W. L. 1984. The rainout parameterization in a photochemical model. *J. Geophys. Res. 90*, 7872–7880.

Hales, J. M. 1982. Mechanistic analysis of precipitation scavenging using a one-dimensional, time-variant model. *J. Atmos. Environ. 16*, 1775–1783.

Hu, Z., and Cai, L. 1979. A parameterized numerical simulation of warm rain and salt-seeding in cumulus clouds. *Scientia Atmospherica Sinica* (in Chinese) *3*, 334–342.

Hu, Z., Yan, C. and Wang, Y. 1983a. Numerical simulation of rain and seeding processes in warm layer clouds. *Acta Meteorologica Sinica* (in Chinese) *41*, 79–88.

Hu, Z., Qin, Y. and Wang, Y. 1983b. A numerical model of the cold stratiform clouds. *Acta Meteorologica Sinica* (in Chinese) *41*, 194–203.

Kessler, E. 1969. On the distribution and continuity of water substance in atmospheric circulations. *Meteorol. Monogr. 10*, 84.

Kins, L. 1982. Temporal variation of chemical composition of rainwater during individual precipitation events. In *Deposition of atmospheric pollutants* (eds. H.-W. Giorgii and J. Pankrath). D. Reidel Publishing Co., Dordrecht, Netherlands, 87–96.

Khrgian, A.Kh. 1961. Editor. *Cloud Physics*. SIMIZ Gidrometeorologicheskoe Izdatel'stvo, Leningrad.

Liu, J. Y. and Orville, H. D. 1969. Numerical modelling of precipitation and cloud shadow effects on mountain-induced cumuli. *J. Atmos. Sci. 26*, 1283–1298.

Marshall, J. S. and Palmer, W. M. 1948. The distribution of raindrops with size. *J. Meteorol. 5*, 165–168.

Mason, B. J. 1960. The evolution of droplet spectra in stratus clouds. *J. Meteorol. 17*, 459–462.

Pruppacher, H. R. and Klett, J. D. 1978. *Microphysics of clouds and precipitation.* D. Reidel Publishing Co., Boston, MA, 714 pp.

Rodhe, H. and Grandell, J. 1981. Estimate of characteristic times for precipitation scavenging. *J. Atmos. Sci. 38*, 370–386.

Sarma, R. A. 1983. Distribution of acidity in convective clouds due to the aqueous-phase oxidation of sulfur dioxide by ozone—a numerical simulation. In *Precipitation scavenging 1*, 617–626.

Silverman, B. and Glass, M. 1973. A numerical simulation of warm cumulus clouds: Part I. Parameterized vs. non-parameterized microphysics. *J. Atmos. Sci. 30*, 1620–1637.

Simpson, J. and Wiggert, V. 1969. Models of precipitating cumulus towers. *Mon. Wea. Rev. 97*, 471–489.

Stewart, R. W., Hameed, S. and Matloff, G. 1983. A model study of the effects of intermittent loss on odd nitrogen concentrations in the lower troposphere. *J. Geophys. Res. 88*, 10697–10707.

Thompson, A. M. and Cicerone, R. J. 1982. Clouds and wet removal as causes of variability in the trace-gas composition of the marine troposphere. *J. Geophys. Res. 87*, 8811–8826.

Zika, R., Saltzman, E., Chameides, W. L. and Davis, D. D. 1982. H_2O_2 levels in rainwater collected in South Florida and the Bahama Islands. *J. Geophys. Res. 87*, 5015–5017.